POLITECNICO DI TORINO
Repository ISTITUZIONALE

Die wear reduction by multifactorial Design of Experiments applied to forging simulations

*Original*
Die wear reduction by multifactorial Design of Experiments applied to forging simulations / Alessio, A., Antonelli, D., Doglione, R., Genta, G.. - ELETTRONICO. - 112:(2022), pp. 424-429. (15th CIRP Conference on Intelligent Computation in Manufacturing Engineering ICME Naples (ITA) July 14-16, 2021) [10.1016/j.procir.2022.09.031].

*Availability:*
This version is available at: 11583/2973351 since: 2022-11-24T09:13:20Z

*Publisher:*
Elsevier

*Published*
DOI:10.1016/j.procir.2022.09.031

*Terms of use:*

This article is made available under terms and conditions as specified in the corresponding bibliographic description in the repository

*Publisher copyright*

(Article begins on next page)

08 October 2026

Available online at www.sciencedirect.com

ScienceDirect

Procedia CIRP 112 (2022) 424–429

www.elsevier.com/locate/procedia

15th CIRP Conference on Intelligent Computation in Manufacturing Engineering, Gulf of Naples, Italy

# Die wear reduction by multifactorial Design of Experiments applied to forging simulations

Alessandro Alessio [a], Dario Antonelli [a]*, Roberto Doglione [b], Gianfranco Genta [a]

[a] *Department of Management and Production Engineering, Politecnico di Torino, Corso Duca degli Abruzzi 24, Torino, Italy*
[b] *INSTM, Via Giuseppe Giusti 9, Firenze, Italy*

* Corresponding author. Tel: +39-011-0907288; fax: +39-011-0907299. *E-mail address:* dario.antonelli@polito.it

**Abstract**

Both wear and fracture mechanisms of 32CrMoV12 dies after hot forging were investigated through SEM and metallographic tests. In order to contain wear mechanisms and to prevent fracture occurrence, a multifactorial Design of Experiments (DoE) has been executed on the Finite Element simulated process. Considered design factors have been limited to process parameters directly modifiable in the actual industrial process. Two step forging cycle has been accounted in the evaluation of stress distribution on the dies and in the estimate of die wear. Despite high process variability, the possibility to effectively hinder fracture and to control most of the wear sources was demonstrated.

© 2022 The Authors. Published by Elsevier B.V.
This is an open access article under the CC BY-NC-ND license (https://creativecommons.org/licenses/by-nc-nd/4.0)
Peer-review under responsibility of the scientific committee of the 15th CIRP Conference on Intelligent Computation in Manufacturing Engineering, 14-16 July, Gulf of Naples, Italy

*Keywords:* Finite element method (FEM), Forging, Design of experiments (DoE).

## 1. Introduction

Hot forging die life prediction is still an open challenge and one of the most coveted in industrial field because tools represent the major cost item for forged components, not considering the annoying slowdowns and machinery downtimes due to tool change. Many attempts were made to correlate Finite Element Method (FEM) simulations and mathematical models of wear to die life to express a universal method which integrates all the factors involved. Achieving a reliable and simple model would simplify engineers' design and optimisation of industrial processes but considering all the factors involved is neither practical nor easy to implement. To avoid this kind of problem it's possible to focus on specific parameters and get anyway the digital twin of the mould used. It is recognized that 70% of dies are discarded due to abrasive wear, 25% due to plastic deformation and the remaining 5% due to cracks caused by thermo-mechanical fatigue, fracture initiation and failure caused by incorrect thermo-chemical treatments [1]. Consequently, analysing plastic deformation and abrasive wear variation in relation to process parameters allow to predict the most significant causes of damage for the die and to find parameter values that optimize die lifespan. In this study, multifactorial Design of Experiments (DoE) was performed (by means of FEM simulations with QForm-3D) to determine the effect of process parameters on die wear and on developed stresses. The analysis has been validated by metallurgical and topological tests on a worn die coming from production.

## 2. Die life optimization

The process parameters involved in hot forging and their role have been subject of investigation by [2]. There is a wide consensus on the application of FEM simulations to optimize process variables, as in [3] or in [4]. In [5] both process and product are optimized concurrently. The complexity of global multi-objective optimization of every factor in the process is so high that several authors prefer to develop empirical expert systems to assist in the design phase [6] or

2212-8271 © 2022 The Authors. Published by Elsevier B.V.
This is an open access article under the CC BY-NC-ND license (https://creativecommons.org/licenses/by-nc-nd/4.0)
Peer-review under responsibility of the scientific committee of the 15th CIRP Conference on Intelligent Computation in Manufacturing Engineering, 14-16 July, Gulf of Naples, Italy
10.1016/j.procir.2022.09.031

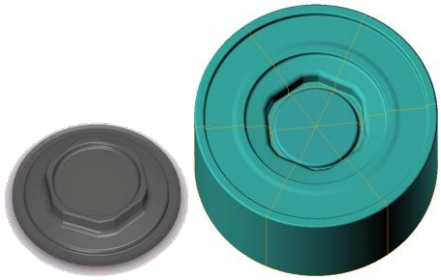

Fig.1 The forged part and the bottom die.

recur to Neural Networks [7] to reduce the number of FEM simulations required.

Among the several aspects of the process that deserve optimization, the increase of die life is the one which impacts more on production costs. Hot forging dies, thus expensive, have a short lifespan reaching 20000 cycles maximum [1]. Die wear mechanisms were investigated in [8] for a common die material, X40CrMoV5-1 steel. FEM simulations leaded to proposals for die life increasing. Present study started from the identification of the wear and failure mechanisms in 32CrMoV12 steel. The wear model has been identified. The significant process factors affecting the die life have been detected using a multi-factorial DoE. The response surfaces have been used to increase the life expectation of the die.

## 3. Identification of damage mechanisms on the die

The case study is the forging of a large nut (Fig.1). The main failure concerns are referred to the bottom die that was analysed at the end of its operating life. In the last version, the die is composite, made up of a central pin shrink fitted on an external ring. Fracture occurred after 7500 cycles.

The limited life span prompted to investigate the causes of the edge fracture, to solve the problem and extending the die life over 7500 cycles limit.

### *3.1. Fracture analysis*

Identifying the primary cause of the fracture is essential to find an effective remedy. Fractographic and metallographic analyses were performed for the damaged part of the die. Thanks to SEM microscope, primary and secondary cracks were identified (Fig.2-a): the former initiate under the surface and propagate parallel to it causing spalling (Fig.2-e), the latter propagate perpendicularly to the surface along the grain boundaries.

Metallographic analyses excluded thermal treatment as the cause of fracture. They also showed (Fig.2-b) a slight nitrided layer where it had not been removed by wear.

From real forged part, an elastic subsidence can be observed between the shrink-fitted elements. The entity of elastic deformation is also apparent in FEM simulations and amounts to a 0.3 millimetres step between the pin and the ring (Fig.2-c). This step is not only an aesthetic defect in the final product but is also responsible for a significant stress intensification on the ring, which is the cause of primary crack.

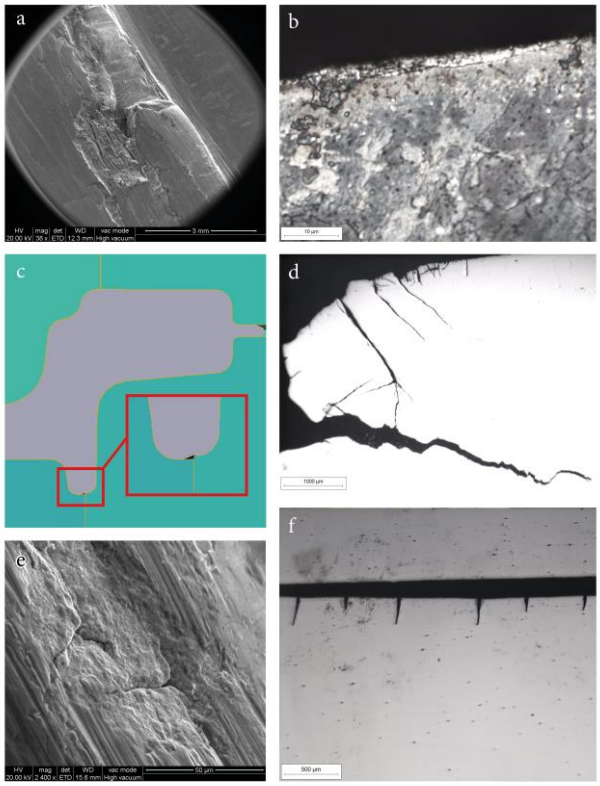


Fig.2 (a) Peeling; (b) Metallographic section: white layer shows residual nitrided film; (c) Elastic subsidence observed in FEM simulations; (d) Example of deep cracks propagation; (e) Detail of spalling phenomenon; (f) Spalling.

Metallographic cross sections also revealed the existence of long cracks (Fig.2-d) initiated from the junction of the hexagonal cavity of the lower ring (Figure 1, inset). This demonstrates heavy loads exceeding those permitted by the material. The metallography performed on the vertical surfaces (in a plane of radial and longitudinal coordinates) also consolidates this conjecture (Fig.2-a): series of recurring cracks are caused by excessive stresses along the longitudinal direction of the die. Nevertheless, not negligible spalling phenomena have been reported (Fig.2-f) which also prove excessive shear stresses [9].

In summary, the die has been nitrided. The layer, originally about 300 µm thick, was almost completely removed during the working cycles. Abnormal operating conditions gave rise to the following phenomena:

- Presence of the step
- Excessive axial stress
- Cracks
- Spalling

### *3.2. Wear analysis*

The worn die silhouette was measured by means of a 3D scanner and then compared with the nominal CAD model (Fig.3). The wear-to-cycle ratio for each point was calculated under the hypothesis that the amount of material worn was the same in every cycle.

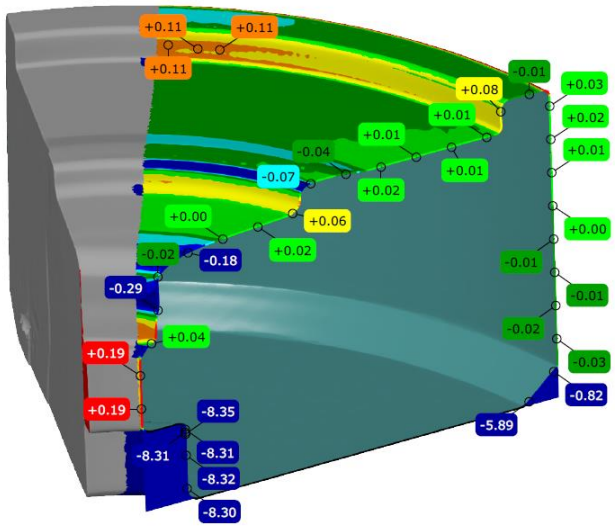


Fig.3 Comparison of scanned 3D surface of the die with CAD model. Positive values in the bottom part are simply due to a production change from the original design

In the study, the well-known Archard model for wear estimation has been used with some adaptations that allow to exploit the detailed knowledge on local stresses on the interface die-workpiece allowed by FEM simulation [11]:

$$W_\tau = K_\tau \int_0^t \frac{\tau v_\tau}{\bar{\sigma}} dt \quad (1)$$

where $W_\tau$ is the wear due to shear stress, $K_\tau$ an empirical coefficient, $v_\tau$ the tangential velocity at the interface between the die and the workpiece, $\tau$ the shear stress at the point of contact, $\bar{\sigma}$ the yield stress of die material, $t$ the contact time between die and workpiece.

The points that have industrial interest are the ones where die wear results in a forged part out of specifications and the ones where the die fractures. They are indicated in Fig.4 indicated as A, B, C and D. Because of difficulties in data acquisition due to the interactions with probe, other points d1, d2, d3, d4, d5 and d6 were acquired in equivalent areas.

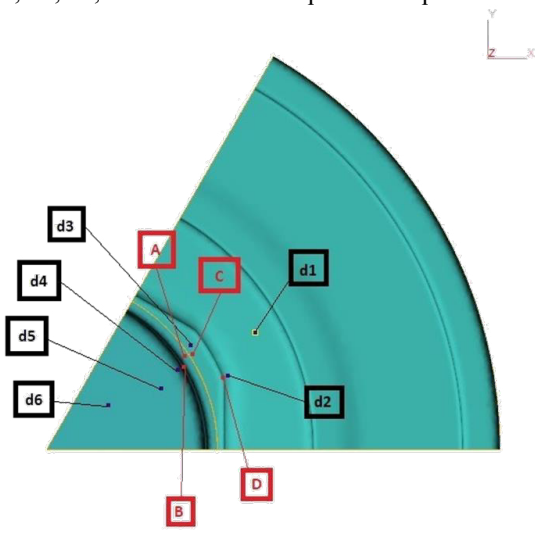


Fig.4 Die points monitored.

Assuming a constant wear-to-cycle ratio, $K_\tau$ was calculated as:

$$K_\tau = \frac{wear_{measured}}{n_{cycles}} \left( \int_0^t \frac{\tau v_\tau}{\bar{\sigma}} dt \right)^{-1} \quad (2)$$

Table 1 shows the results for points with measurable wear. Values are scattered, due to the very low wear of some considered points, but for the most worn points, C, D and d2 they are in good agreement.

Table 1. $K_\tau$ values in the points with measurable wear

| Point | Wear measured [mm] | $wear/cycles_{me.}$ [mm/cycle] | $wear/cycles_{sim.}$ [mm/cycle] | $K_\tau$ |
|---|---|---|---|---|
| C | 0,16 | 2,13E-05 | 7,03E-05 | 0,30 |
| D | 0,16 | 2,13E-05 | 6,01E-05 | 0,35 |
| d1 | 0,03 | 4,00E-06 | 3,13E-05 | 0,13 |
| d2 | 0,18 | 2,40E-05 | 7,07E-05 | 0,34 |
| d3 | 0,08 | 1,07E-05 | 5,12E-05 | 0,21 |

## 4. Identification of production factors affecting die life

DoE analysis allows to determine the dependence of output variables from input factors and their mutual interactions. A campaign of experiments allows to understand which are the significant production factors and to predict the consequences of their variation on the process outcomes.

The analysis of variance (ANOVA) applied to a DoE allows to distinguish the amount of variation caused by inputs under control and by random errors through the parameters $R^2$ and p-value. $R^2$ represents the goodness of regression equation fit, while p-value is used to evaluate the significance of input factors and their mutual interactions.
The main difference between simulated and experimental DoE is that in the first case the replications of the experiments are not needed.

### *4.1. Choice of production factors*

In this study a full factorial plan of experiments was simulated with QForm-3D software. The factors were chosen among the ones that would have been actually modifiable by the factory during the production. The levels of every factor depend on the expected shape of response surface. As the response surface is expected to be nonlinear, it deemed necessary to have 3 levels for every factor. Eventually, 3 factors are considered with 3 levels each, for a total amount of 27 trials. Factors that can be easily varied in actual industrial process are: die pre-heating temperature ($T$), lubricant type ($m$) and billet height after the upsetting operation ($h$).

Manufacturing constraints limit billet height in the range 16-20 mm. Die temperature reduces forming stresses and thermal fatigue so increasing this parameter is recommended. However, the thermal softening can lead to a

faster abrasive wear and plastic deformation of the tool. Practice suggests a value of 300 °C in a range between room temperature (20 °C) and a maximum 400 °C.

Lubricants have several effects on the process, but their main role is friction reduction. Levanov's friction model was adopted:

$$\tau_{\text{Levanov}} = \mathrm{m}\frac{\bar{\sigma}}{\sqrt{3}}\left(1 - \mathrm{e}^{-\mathrm{n}\frac{\sigma_n}{\bar{\sigma}}}\right) \quad (3)$$

where $m$ is the friction factor, $\bar{\sigma}$ the yield stress of the workpiece, $\sigma_n$ the normal stress at the point of contact, $n$ the Levanov coefficient (in this case 1.25). In order to extend the friction factor variability, the best available lubrication ($m$=0.15) and its absence ($m$=0.8) were chosen as extreme conditions. Factors and levels are summarized in Table 2.

Table 2. The selected factors and their levels

| Factor | Minimum | Intermediate | Maximum |
|---|---|---|---|
| Initial die Temperature [°C] | 20 | 210 | 400 |
| Workpiece height [mm] | 16 | 18 | 20 |
| Friction factor [-] | 0.15 | 0.4 | 0.8 |

### *4.2. Choice of output variables*

The damaging causes identified on the die are some and therefore different outputs must be monitored: average die stress, equivalent stress and abrasion wear. Fracture occurrence is one off, therefore it has been substituted by average stress that is an indicator of fracture probability.
The average tension is expressed by the following equation:

$$\sigma_{average} = \frac{\sigma_{ii}}{3} \quad (4)$$

where $\sigma_{ij}$ is the stress tensor. Plastic deformation of the die occurs whenever the material yield strength is exceeded and can lead to unacceptable unconformities in the shape of the final product. Yield strength reduces with temperature so, those areas of the die where it increases due to the contact with the workpiece, can incur local plastic deformation. The closeness to the yield stress is monitored through the equivalent stress according to the Von Mises criteria:

$$\bar{\sigma} = \sqrt{\frac{3}{2}\sigma_{ij}\sigma_{ij}} \quad (5)$$

Abrasion wear is calculated by (1) with the wear coefficient identified in Table 1 (average 0.3 was adopted).

### *4.3. Analysis of results*

The analysis was focused on the bottom die as the more subjected to failure and wear. A first attempt with first order linear regression analysis obtained very low values of $R^2$ and was discarded. Second order regression models were searched for each point in the following form:

$$\mathrm{y} = \mathrm{const} + \beta_i x_i + \beta_{ij} x_i x_j \quad (6)$$

where *const* is the intercept of the model, $x_i, x_j$ the independent variables, $\beta_i$ the coefficients of first order terms, $\beta_{ij}$ the coefficients of second order terms. Coefficient values were calculated using Minitab software. Examined points are specified in Fig.4. Significant and non-significant models are summarised in Table 3. In every model, only some variables or interactions are significant.

Table 3. Significant and non-significant models obtained

| Point | Average stress model | Equivalent stress model | Wear model |
|---|---|---|---|
| A | NO | NO | NO |
| B | NO | YES ($R^2$=95.48%) | NO |
| C | NO | YES ($R^2$=89.22%) | NO |
| D | YES ($R^2$=84.30%) | YES ($R^2$=92.06%) | YES ($R^2$=96.99%) |
| d1 | YES ($R^2$=87.80%) | YES ($R^2$=92.75%) | YES ($R^2$=97.57%) |
| d2 | YES ($R^2$=91.78%) | YES ($R^2$=92.07%) | NO |
| d3 | NO | NO | NO |
| d4 | YES ($R^2$=89.82%) | YES ($R^2$=98.43%) | YES ($R^2$=94.93%) |
| d5 | YES ($R^2$=90.13%) | YES ($R^2$=99.39%) | YES ($R^2$=99.90%) |
| d6 | NO | YES ($R^2$=98.66%) | YES ($R^2$=99.71%) |

Low $R^2$ in simulations is attributed to:

- interpolation errors introduced by automatic remeshing;
- die deformation, changing the position of stress concentrations with respect to the points chosen on the undeformed model;
- alternating traction and compression stress in the outer die: the interference fit produces an initial tensile state in the outer die. During the forging, stress state reverts in different process times.

The significance of production factors has been assessed by their p-values for every point and for every output. With some exceptions, the significance order is often: friction coefficient ($m$), billet height ($h$) and die temperature ($T$). Strong variations have been noted between zones of different orientation, for example comparing horizontal surfaces to vertical ones. For this reason, point D which is the only one located on a vertical surface of the die describes the general behaviour differently from the rest of the points.

Analysing the mean stress, main effect graphs referred to the vertical surface of the hexagon (point D) showed remarkable non-linearities in relation to the friction factor and the billet height (Fig.5-a). For the rest of the mould (points d1, d2, d4 and d5) the behaviour is uniform: the mean stress modulus decreases as the die temperature and the billet height increase, opposite trend is obtained for greater friction factor values. Interaction plots for average stress confirm the previous results and show the positive effect of increasing die temperature as the lubricant efficiency decreases, an example is shown in Fig.5-b.

Analysing the effective stress, main effects plots showed similar behaviour in all areas of the mould (Fig.5-c) with the only exception for the area subjected to fracture: general

trends revealed the most significant influence in friction factor (points B, D, d1, d2, d4, d5 and d6), whereas for the zone subjected to fracture (point C) billet height was the most significant one (Fig.5-d).

Coming to abrasive wear, plots show that the mould reacts in different way depending on the surface analysed: the same trends (Fig.5-f) were noted for horizontal surfaces and the outward curvature radii, whereas trends for vertical surfaces of the hexagon (point D) were different (Fig.5-e). It is generally true that wear increases as the lubrication quality decreases and it is barely affected by initial die temperature. Wear relationship related to the billet height is negative for the vertical surfaces (point D) and positive for the rest of the mould.

Interaction plots show different responsiveness in relation to the different operating conditions (Fig.5-g). As a consequence, they allow to identify threshold values for input factors to reduce maximum wear and stress.

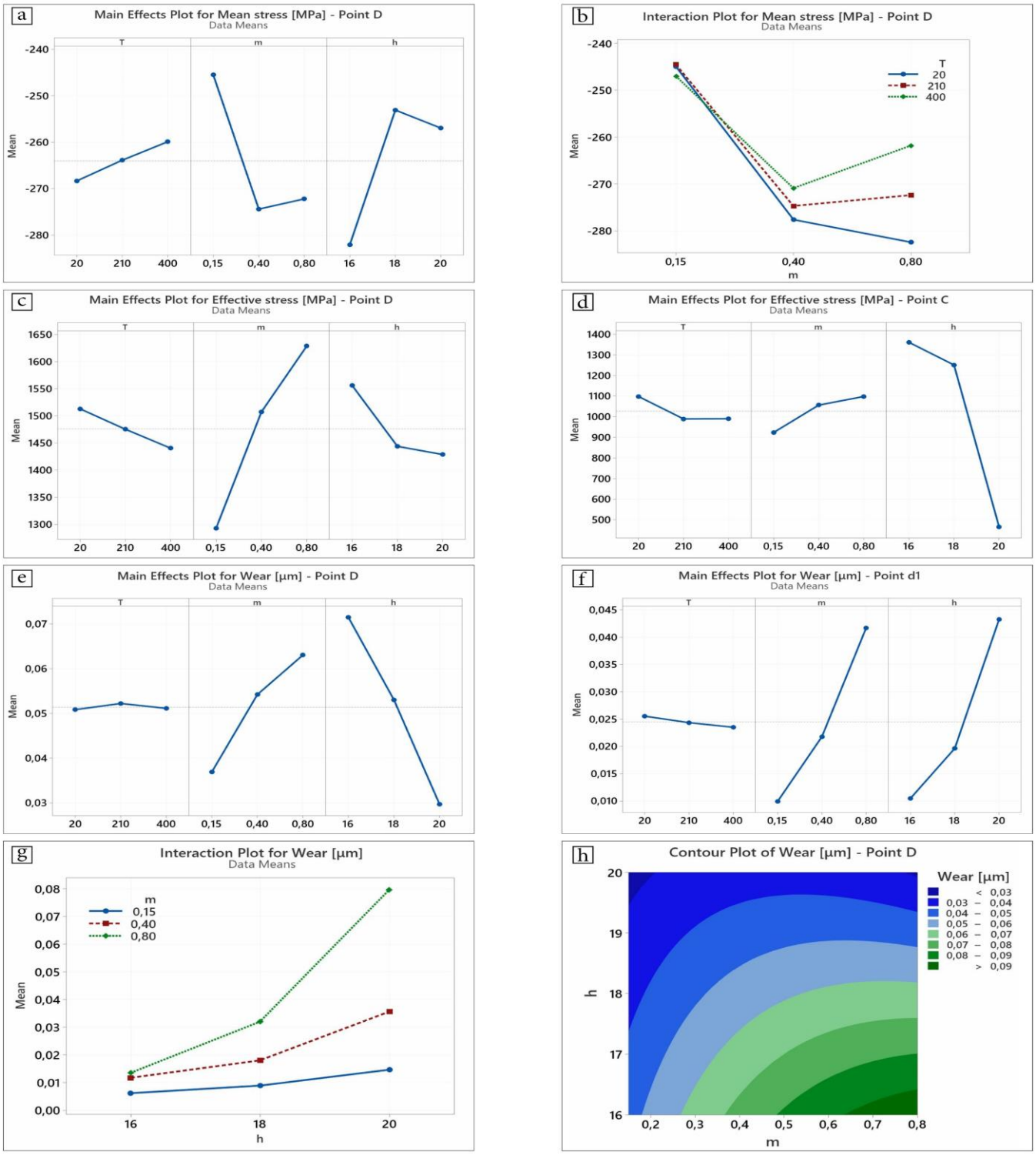


Fig.5 (a) Mean stress trends for vertical surfaces; (b) example of positive effect of increasing die temperature as the lubricant efficiency decreases; (c) typical effective stress trend; (d) effective stress trend in zone subjected to fracture; (e) wear trend for vertical surfaces; (f) typical wear trend; (g) example of threshold value for parameter *h* ; (h) contour plots of wear for vertical surfaces.

## 5. Die life prediction

An outcome of DoE analysis is that die life optimization depends more on friction coefficient and billet height than on die temperature. Contour plots describe stress and wear trends (see, e.g., Fig.5-h) as the input parameters change and help to determine the best setup easily. The general optimum setup varies with the choice of the damage mechanism to control: to reduce stress a higher billet is preferred whereas to reduce wear a lower one is best; in both cases higher die temperature are preferred as well as lubrication quality (minimum *m*). There are exceptions as point D (the one on a vertical surface) and d4 (on outward curvature radius) showed minimum wear for the highest value of billet height. Optimised parameters are given in Table 4.

Table 4. Optimised parameter

| Model | Point(s) | T [°C] | m | h [mm] |
|---|---|---|---|---|
| Average stress | B | - | 0,15 | - |
| | D | 400 | 0,15 | 18,42 |
| | d1, d2, d4, d5 | 400 | 0,15 | 20 |
| Effective stress | C | 400 | 0.8 | 20 |
| | D | 400 | 0,15 | 19,84 |
| | d1, d2 | 400 | 0,15 | 20 |
| | d4 | - | 0,15 | 20 |
| | d5 | 400 | 0,15 | 19,19 |
| | d6 | 400 | 0,15 | 19,60 |
| Wear | D, d4 | - | 0,15 | 20 |
| | d1 | - | 0,15 | 17,62 |
| | d5, d6 | 400 | 0,15 | 16 |

To optimize die life two actions are required: prevent the insurgence of fracture and contain the two main damage mechanisms: wear and plastic deformation. As in all simulations, plastic deformation did not occur, the process was optimized only for abrasive wear containment.

Prevention of primary cause of fracture is obtained by different assembly of composite die that compensate elastic subsidence.

Acceptable wear threshold on the most critical surface (point D), according to design requirements for the part, is 0.43 mm. From the wear model obtained in point D and using the company's parameters the estimated wear-per-cycle is 2.13E-05 mm/cycle which allows 9986 working cycles. Adopting the optimised factors of Table 4, maximum die life can be extended up to 22156 cycles. This is the optimum value since the calculus does not consider the actual wear rate progression: it is expected a sharp increase in the wear rate with the removal of last layers of nitride coating. But even so, the optimization could bring considerable economic benefits.

## 6. Conclusions

Predicting hot forging die life is still object of research. The reasons are in the multitude of factors involved, some of them out of control during the process. However, the main phenomena causing die discard are known and this study has shown that it is possible to limit their effects and retard them as much as possible.

In this study, the focus was on plastic deformation and abrasive wear, so that models widely adopted in literature have been used. Even though it is difficult to test on the field all the optimizations proposed, just a subset of optimization results can provide considerable increase of die lifespan.

Further development of this work will consist in replacing the response surface, needed for adequate data fit, with kriging regression. It will allow to thicken the simulations around expected optimum. Another significant improvement will be adding in the DoE the main disturbance factors, i.e., the process parameters that are not controllable, whose variation can affect the quality of results. The main disturbance factors are the initial billet volume and the time between consecutive strokes. The first determines the amount of material flowing in the flash. The second influences both workpiece and die temperature.

## 7. References

[1] Gronostajski, Z., Kaszuba, M., Hawryluk, M., & Zwierzchowski, M. (2014). A review of the degradation mechanisms of the hot forging tools. Archives of Civil and Mechanical Engineering, 14(4), 528-539.

[2] Kim, D. H., Lee, H. C., Kim, B. M., & Kim, K. H. (2005). Estimation of die service life against plastic deformation and wear during hot forging processes. Journal of Materials Processing Technology, 166(3), 372-380.

[3] António, C. C., Castro, C. F., & Sousa, L. C. (2004). Optimization of metal forming processes. Computers & structures, 82(17), 1425-1433.

[4] Vazquez, V., & Altan, T. (2000). Die design for flashless forging of complex parts. Journal of Materials Processing Technology, 98(1), 81-89.

[5] Ozturk, M., Kocaoglan, S., & Sonmez, F. O. (2016). Concurrent design and process optimization of forging. Computers & Structures, 167, 24-36.

[6] Kulon, J., Mynors, D. J., & Broomhead, P. (2006). A knowledge-based engineering design tool for metal forging. Journal of Materials Processing Technology, 177(1), 331-335.

[7] DAddona, D. M., & Antonelli, D. (2018). Neural Network Multiobjective Optimization of Hot Forging. Procedia CIRP, 67, 498-503.

[8] Kchaou, M., Elleuch, R., Desplanques, Y., Boidin, X., & Degallaix, G. (2010). Failure mechanisms of H13 die on relation to the forging process–A case study of brass gas valves. Engineering Failure Analysis, 17(2), 403-415.

[9] Failure Analysis and Prevention, ASM Handbook, Volume 11, pp. 975, 982, ASM International, 2002.

[10] Bonte, M. H., Fourment, L., Do, T. T., Van den Boogaard, A. H., & Huetink, J. (2010). Optimization of forging processes using Finite Element simulations. Structural and Multidisciplinary optimization, 42(5), 797-810.

[11]Andersson, J., Almqvist, A., & Larsson, R. (2011). Numerical simulation of a wear experiment. Wear, 271(11-12), 2947-2952.